16

CP violation: D and B mesons

16.1 Introduction

In previous chapters we mentioned that the analysis of bound states with heavy quarks varies from meson to meson. For heavy mesons the hadronic structure becomes simpler and approaches the spectator model with corrections given by HQET. Their weak properties, on the other hand, remain distinct because they depend on the interplay between CKM couplings and the masses of the mesons. For this reason we discuss the mixing and CP violation in D and B mesons in a separate chapter.

The system D^0–$\bar{D}^0$ is quite different because the decay width is much larger than the mass and width differences, which makes the observation of mixing and of CP asymmetries very difficult. In fact, they have not been observed yet. This motivated several authors to suggest that the observation of these effects, at a higher level than expected, will be an indication of contributions beyond the standard model.

The observation of these effects in the neutral B mesons was experimentally promising because the decay of the b quark to its heavier partner, the top quark, is not possible for kinematic reasons. The suppressed decay width is comparable to the difference in mass of the B_d mesons. Consequently, the mixing over their lifetimes is substantial and has been observed. In addition, the mixing of the states provides another phase that interferes with phases of decay amplitudes and produces oscillations observable in the experiments. These are some of the topics to be covered in this chapter.

16.2 The D^0–$\bar{D}^0$ transition amplitude

The calculation of the mass difference for K_S and K_L mesons in terms of the box diagrams gave a sizable fraction ($\geq$50%) of the observed value. This suggests that similar calculations for heavier mesons may be more accurate. Indeed, estimates of ΔM and $\Delta\Gamma$ for D^0 mesons give small values relative to the decay width of these

https://doi.org/10.1017/9781009402378.017 Published online by Cambridge University Press

particles. For this reason, mixing of the neutral D states and CP asymmetries have not yet been observed. Similar calculations for the B mesons give values consistent with the data, because box diagrams are dominated by top quarks in the intermediate states.

As mentioned in Section 14.7, mixing of states depends on the size of the decay width relative to the value of the off-diagonal matrix elements of the effective Hamiltonian. We can estimate both of these terms for D mesons. The decay width in the spectator model is given approximately by

$$\Gamma = \frac{G^2 m_c^5}{192\pi^3}|V_{cs}|^2. \tag{16.1}$$

This should be compared with the following matrix element of the effective Hamiltonian:

$$\begin{aligned}\langle \bar{D}^0|H_{12}|D^0\rangle = &-\frac{G^2}{16\pi^2}M_W^2\left[\xi_s^2 E(x_s) + 2\xi_s\xi_b E(x_s,\ x_b) + \xi_b^2 E(x_b)\right] \\ &\times\langle \bar{D}^0|\bar{c}\gamma_\mu(1-\gamma_5)u\bar{c}\gamma^\mu(1-\gamma_5)u|D^0\rangle.\end{aligned} \tag{16.2}$$

The factors $\xi_s = V_{us}^* V_{cs}$ and $\xi_b = V_{ub}^* V_{cb}$ are given in terms of Kobayashi–Maskawa matrix elements, which in the Wolfenstein parametrization are of order λ and λ^5, respectively. The $E(x_s)$ and $E(x_b)$ pertain to strange and bottom quarks and are approximated for $m_i^2 \ll M_W^2$ by

$$E(x_i) \approx -x_i. \tag{16.3}$$

The reduced matrix element

$$X_D = \langle \bar{D}|\bar{c}_\alpha\gamma_\mu(1-\gamma_5)u_\alpha\bar{c}_\beta\gamma^\mu(1-\gamma_5)u_\beta|D\rangle, \tag{16.4}$$

with α and β color indices, is similar to the matrix element encountered for K mesons in Section 15.4. An order-of-magnitude estimate is given by the vacuum-insertion approximation, which consists of introducing the vacuum state in all possible ways. For the above case we obtain

$$\begin{aligned}X_D &= \langle \bar{D}|\bar{c}_\alpha\gamma_\mu(1-\gamma_5)u_\alpha|0\rangle\langle 0|\bar{c}_\beta\gamma_\mu(1-\gamma_5)u_\beta|D\rangle \\ &\quad + \langle \bar{D}|\bar{c}_\alpha\gamma_\mu(1-\gamma_5)u_\beta|0\rangle\langle 0|\bar{c}_\beta\gamma_\mu(1-\gamma_5)u_\alpha|D\rangle \\ &= \left(1+\frac{1}{3}\right)|\langle \bar{D}|\bar{c}_\alpha\gamma_\mu(1-\gamma_5)u_\alpha|0\rangle|^2 \\ &= \frac{8}{3}F_D^2 M_D.\end{aligned} \tag{16.5}$$

The second equation is obtained by Fierzing the second and the fourth spinors and the factor of $\frac{1}{3}$ by transforming the matrix elements to color singlets (use

https://doi.org/10.1017/9781009402378.017 Published online by Cambridge University Press

Eq. (15.88)). The decay coupling constant is defined as

$$\langle 0|\bar{c}_{\rm L}\gamma_\mu u_{\rm L}|D\rangle = {\rm i}\frac{F_{\rm D}\, p_\mu}{\sqrt{2M_{\rm D}}}, \tag{16.6}$$

with $u_{\rm L}$ being a normalized left-handed spinor.

It is straightforward to estimate ratios of the mass and width differences to the width. The b-quark exchange graphs are smaller than that for the strange-quark exchange, because of the very small b coupling. Estimates of the strange-quark graph give

$$x = \frac{\Delta M}{\Gamma} \approx O(10^{-4}) \qquad \text{and} \qquad y = \frac{\Delta\Gamma}{2\Gamma} \approx O(10^{-4}), \tag{16.7}$$

with more precise estimates depending on values for the parameters. Alternatively, one may use hadronic intermediate states, but very few amplitudes are known at present and their phases are unknown. The above values of x and y give very small mixing.

Since the lifetime of D mesons is very short, only time-integrated effects can be observed. They are defined in terms of the transition probabilities $|\langle\bar{D}^0|D^0(t)\rangle|^2$ and $|\langle D^0|D^0(t)\rangle|^2$, whose functional forms in terms of widths and masses are similar to those for the K mesons given at the end of Section 15.3:

$$\begin{aligned} r &= \frac{\int_0^\infty |\langle\bar{D}^0|D^0(t)\rangle|^2}{\int_0^\infty |\langle D^0|D^0(t)\rangle|^2} = \left|\frac{q}{p}\right|^2 \frac{\int |f_-(t)|^2\,{\rm d}t}{\int |f_+(t)|^2\,{\rm d}t} \\ &= \left|\frac{q}{p}\right|^2 \frac{\Delta M^2 + (\Delta\Gamma/2)^2}{2\Gamma^2 + (\Delta M)^2 - (\Delta\Gamma/2)^2} = \left|\frac{q}{p}\right|^2 \frac{x^2+y^2}{2+x^2-y^2}. \end{aligned} \tag{16.8}$$

These equations imply that the expected mixing for neutral D mesons for the values in (16.7) will be of order 10^{-8} and any observable mixing must be attributed to another mechanism beyond the standard model.

Even though the estimates for $\rm D^0$ are very approximate, the methods we described in this section are general and can be taken over for other mesons. The vacuum-insertion approximation of Eq. (16.5) has already been used for K mesons and we will meet it again in the next section. Vacuum insertion is an approximation that several authors tried to improve. It is hoped that lattice gauge theories will eventually give precise values.

The second result of this section, Eq. (16.8), gives the mixing of short-lived states integrated over long intervals of time. This is a general result that depends on the quantum-mechanical development of a two-state system. In a tagged $\rm D^0$ beam, the ratio r gives the number of wrong-sign leptons produced in the decays divided by the number of right-sign leptons. The wrong-sign leptons are those which originate from the oscillation of $\rm D^0$ to $\rm \bar{D}^0$ mesons. We mentioned leptons as an example, but

https://doi.org/10.1017/9781009402378.017 Published online by Cambridge University Press

they can be substituted by decays into K mesons of specific strangeness. Such a ratio was in fact used to determine B^0–$\bar{B}^0$ mixing, which we shall explain in Section 16.4.

16.3 Comparison of K^0 and B^0 mesons

It is instructive at the very beginning to compare several properties of the K^0 and B^0 mesons, because these two mesons are quite different. For the K mesons there are two physical states with very different lifetimes:

$$\tau(K_S) = 89.35\,\text{ps} \qquad \text{and} \qquad \tau(K_L) = 51\,700\,\text{ps}. \tag{16.9}$$

This big difference comes about because the mass and width differences of the K mesons are comparable:

$$\Delta M_K = -\frac{1}{2}\,\Delta\Gamma_K = -\frac{1}{2}\Gamma_s. \tag{16.10}$$

For the B mesons the situation is very different. The lifetime of the B mesons is much smaller:

$$\tau(B) = 1.55 \pm 0.06\,\text{ps}. \tag{16.11}$$

In addition $\Gamma_{12} \ll M_{12}$ for B_d mesons, which makes the lifetimes of the two physical states almost identical. For this reason we characterize them by their masses, as heavy and light, and denote them by B_H and B_L, respectively. From the mixing of the two states we know the ratio

$$\frac{\Delta M}{\Gamma} = 0.73 \pm 0.18. \tag{16.12}$$

The mixing of the B states is described by box diagrams analogous to those in Fig. 14.4, with the top quark dominating in the intermediate states. Computation of the diagrams gives the mixing parameter, ε_B, as

$$\frac{q}{p} = \frac{1-\varepsilon_B}{1+\varepsilon_B} \approx \frac{V_{td}}{V_{td}^*} = e^{-2i\beta}, \tag{16.13}$$

with β the phase of the V_{td}^* matrix element; see Eq. (16.27). It follows from this relation that ε_B is mostly imaginary with a small real part. Consequently, the leptonic asymmetry that was useful in K decays is too small, so another method for observing CP violation has had to be discovered.

Among the interesting phenomena are the mixing of B_d states and CP asymmetries which have been observed in decays of these mesons. It is mathematically easier to discuss the CP asymmetry because it deals with the time development for single states $|B^0(t)\rangle$ and $|\bar{B}^0(t)\rangle$. The mixing, on the other hand, observes the

https://doi.org/10.1017/9781009402378.017 Published online by Cambridge University Press

correlated development of two states and its calculation is more complicated. Historically, mixing was observed first and the CP asymmetries were observed only very recently. We shall follow the historical development and describe first the mixing of B_d^0 and $\bar{B}_d^0$ states. So far we have mentioned B_d states as typical mesons because experimental results on their decays are available. There are also the B_s mesons, which are very interesting because several of the parameters are different. We postpone a comparison of B_s and B_d states until Section 16.6.

16.4 Mixing in the B_d system

The mixing between B_d and $\bar{B}_d$ mesons was discovered in electron–positron collisions in which a B^0–$\bar{B}^0$ pair is produced. As the produced pair develops in time, the particles oscillate. The time development of each state separately is given by the following equations. A state that starts as $|B^0(t=0)\rangle$ develops according to

$$|B^0(t)\rangle = N\left[f_+(t)|B^0\rangle + \frac{q}{p}\, f_-(t)|\bar{B}^0\rangle\right]. \tag{16.14}$$

Similarly, a state that starts as $|\bar{B}^0(t=0)\rangle$ develops as

$$|\bar{B}^0(t)\rangle = N\left[\frac{p}{q}\, f_-(t)|B^0\rangle + f_+(t)|\bar{B}^0\rangle\right], \tag{16.15}$$

with

$$f_\pm(t) = \mathrm{e}^{-\mathrm{i}(M_\mathrm{H}-\mathrm{i}\Gamma_\mathrm{H}/2)t} \pm \mathrm{e}^{-\mathrm{i}(M_\mathrm{L}-\mathrm{i}\Gamma_\mathrm{L}/2)t}. \tag{16.16}$$

and N the normalization factor. To describe the oscillation data properly, we must use quantum-mechanical wave functions for a B^0–$\bar{B}^0$ pair. The pair of B mesons created at the Y(4S) resonance is a state with odd charge conjugation with the two mesons flying apart from each other with momenta $\vec{k}$ and $-\vec{k}$. The oscillations that set in are highly correlated. The time evolution of the pair is now given by

$$|B^0(t),\ \vec{k}\rangle|\bar{B}^0(t'),\ -\vec{k}\rangle - |\bar{B}^0(t),\ \vec{k}\rangle|B^0(t'),\ -\vec{k}\rangle. \tag{16.17}$$

It is evident that the decays can take place at different times, with the production of leptons through semileptonic decays. For example, we can consider events of the type

$$\begin{array}{ccccc} \mathrm{e^+e^-} \longrightarrow & \mathrm{B^0} & & + \bar{\mathrm{B}}^0 & \\ & \hookrightarrow \mathrm{Y^+\ell^-\bar{\nu}} & & \hookrightarrow \mathrm{X^-\ell^+\nu} & \\ & \text{or } \mathrm{X^-\ell^+\nu} & & \text{or } \mathrm{Y^+\ell^-\bar{\nu}}. & \end{array} \tag{16.18}$$

Consequently, events are produced in which the pairs of primary leptons emitted are $\ell^+\ell^+$, $\ell^+\ell^-$, $\ell^-\ell^+$, and $\ell^-\ell^-$. We denote the corresponding rates by l^{++}, l^{+-}, l^{-+},

https://doi.org/10.1017/9781009402378.017 Published online by Cambridge University Press

and l^{--}, respectively. The observation of the parameter

$$R \equiv (l^{++} + l^{--})/(l^{+-} + l^{-+}) \tag{16.19}$$

characterizes particle–antiparticle mixing. We denote by A^{--} the amplitude that one of the mesons with momentum $-k$ decays at time t' into ℓ^- and the other meson decays at time t also to ℓ^-. Using the time dependence of the $|B^0(t)\rangle$ and $|\bar{B}^0(t)\rangle$ states given explicitly in Eqs. (16.14) and (16.15), we obtain for the amplitude A^{--}

$$A^{--}(t', t) = \langle \ell^- Y^+ | H | B^0, -k \rangle \langle \ell^- Y^+ | H | B^0, +k \rangle (p/q)[f_-(t')f_+(t) - f_+(t')f_-(t)], \tag{16.20}$$

and, in the same notation,

$$A^{-+}(t',\ t) = \langle \ell^- Y^+ | H | B^0,\ -k \rangle \langle \ell^+ X^- | H | \bar{B}^0,\ +k \rangle \big[f_-(t')f_-(t) - f_+(t')f_+(t) \big]. \tag{16.21}$$

There are two more equations defining the amplitudes $A^{+-}(t',\ t)$ and $A^{++}(t',\ t)$, Paschos and Türke, 1989, p. 218).

For the matrix elements, we introduce the abbreviations

$$\mathcal{M} = \langle \ell^- Y^+ | H | B^0,\ \pm k \rangle, \qquad \bar{\mathcal{M}} = \langle \ell^+ X^- | H | \bar{B}^0,\ \pm k \rangle,$$

which, according to CPT symmetry, satisfy

$$|\mathcal{M}| = |\bar{\mathcal{M}}| = M. \tag{16.22}$$

It is easy to calculate the rates of decay to each pair of charges by squaring the amplitudes and integrating over the times t and t', separately. After some algebra and a few integrations, the final answer is

$$R = \frac{1}{2}\left(\left| \frac{q}{p} \right|^2 + \left| \frac{p}{q} \right|^2 \right) \frac{x^2 + y^2}{2 + x^2 - y^2}, \tag{16.23}$$

with x and y defined for B mesons with $\Delta M = M_{\mathrm{H}} - M_{\mathrm{L}}$ and $\Delta\Gamma = \Gamma_{\mathrm{H}} - \Gamma_{\mathrm{L}}$. It is interesting to note that Eq. (16.23) is similar in many respects to Eq. (16.8).

Experiments measured the ratio in $\mathrm{e}^-\mathrm{e}^+$ collisions and found

$$R = 0.23 \pm 0.09 \pm 0.03. \tag{16.24}$$

For $|q/p| = 1$ and $y \ll 1$, which will be shown later to be an excellent approximation,

$$\frac{\Delta M}{\Gamma} = 0.73 \pm 0.18. \tag{16.25}$$

It is now a theoretical problem to calculate ΔM and $\Delta\Gamma$ for the B system and compare it with the above values.

https://doi.org/10.1017/9781009402378.017 Published online by Cambridge University Press

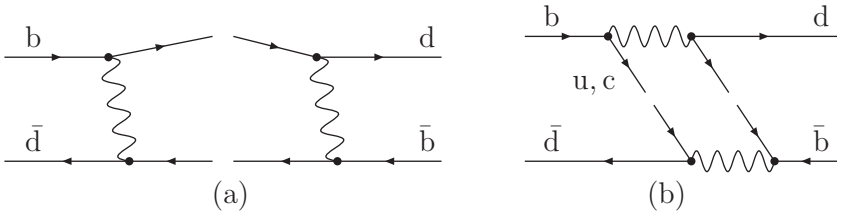

Figure 16.1. Absorptive parts contributing to the B^0–$\bar{B}^0$ width mixing.

The mass difference is given by the box diagrams. Estimates similar to those of the previous sections indicate that the B^0–$\bar{B}^0$ transition amplitude is dominated by the exchange of two top quarks in the box diagram. This is indeed a short-distance contribution. Formula (15.48) translates into

$$M_{12} = -\frac{G^2}{16\pi^2} M_W^2 X_B \xi_t^2 E(x_t)\tilde{\eta}, \tag{16.26}$$

with

$$\xi_t = V_{tb}V_{td}^* = A\lambda^3(1-\rho-i\eta), \tag{16.27}$$

$$X_B = \langle B_0|\,\bar{b}\gamma_\mu(1-\gamma_5)d\bar{b}\gamma^\mu(1-\gamma_5)d|\bar{B}_0\rangle, \tag{16.28}$$

and $\tilde{\eta} \approx 0.87$ is a factor originating from QCD corrections. The reduced matrix element is parametrized in terms of the vacuum-insertion term times a B factor,

$$X_B = \frac{8}{3}|\langle B^0|\,\bar{b}\gamma_\mu(1-\gamma_5)d|0\rangle|^2 B_b = \frac{8}{3}F_B^2 M_B B_b. \tag{16.29}$$

The factor $\frac{8}{3}$ originates from the various terms in the product of the currents and rearrangement of the color indices, as was explained in Section 16.2.

Before we consider the magnitude of the mass difference, it will be useful to calculate the width difference computed as the absorptive part of the box diagrams.

For the calculation of the absorptive part we set the intermediate states on the mass shell. This is equivalent to cutting the diagrams in the manner shown in Fig. 16.1 and then integrating over the two-body phase space.

After completion of the integrations and substitution of the reduced matrix element from Eq. (16.29), one obtains (Hagelin, 1981)

$$\Gamma_{12} \simeq -\frac{G^2 m_b^2}{8\pi} F_B^2 M_{B_d} B\left[(\xi_c+\xi_u)^2 - \frac{8}{3}\frac{m_c^2}{m_b^2}\left(\xi_c^2+2\xi_c\xi_u\right) + O\left(\frac{m_c^4}{m_b^4}\right)\right]. \tag{16.30}$$

This is a relatively simple formula, which can be compared with M_{12}. Neglecting terms of order $(m_c/m_b)^2$, we observe that Γ_{12} has the same phase as M_{12}. This is

https://doi.org/10.1017/9781009402378.017 Published online by Cambridge University Press

evident from the unitarity of the Kobayashi–Maskawa matrix, which gives

$$\xi_u + \xi_c = -\xi_t \tag{16.31}$$

and consequently

$$\Gamma_{12} = -\frac{G^2 m_b^2}{8\pi} F_{B_d}^2 M_{B_d} B \xi_t^2. \tag{16.32}$$

Whenever M_{12} and Γ_{12} have the same phase,

$$\frac{q}{p} = \left(\frac{M_{12}^*}{M_{12}}\right)^{\frac{1}{2}} = \frac{V_{td}}{V_{td}^*} = e^{-2i\beta}, \tag{16.33}$$

as was already given in Eq. (16.13). This ratio will be important for the discussion of CP violation.

A second consequence is the magnitude of Γ_{12} relative to M_{12}:

$$\frac{\Gamma_{12}}{M_{12}} \approx 6\pi \left(\frac{m_b}{m_t}\right)^2 \approx 10^{-2}. \tag{16.34}$$

Numerical estimation of the mass difference gives the value $\Delta M \approx 0.73\Gamma$, in agreement with the mixing of the B^0 and $\bar{B}^0$ states.

16.5 Decay rates and CP violation

B-meson decays are frequently described in terms of quark diagrams, which are classified as tree, penguin, or other types of diagrams. The classification is very useful since it specifies how the CP phases appear in amplitudes, that is as couplings of the CKM-matrix elements. The detailed dynamics are not completely understood and we presented several methods for analyzing them in Chapter 14.

In the spectator model, the simplest diagrams for the decay of a $\bar{b}$ involve only one intermediate W^+ boson, as shown in Fig. 16.2.

We denote the decays of the W^+ boson as $u\bar{d}$ or $c\bar{s}$ and we indicate in closed ovals the final hadronic states. Thus the diagrams (a) denote the decays

$$B_d \to D_s^+ D_d^- \qquad \text{or} \qquad B_d \to \pi^+ D_d^-, \tag{16.35}$$

with the couplings $V_{cb}^* V_{cs}$ and $V_{cb}^* V_{ud}$, respectively. Similarly, the decays in diagram (b) are

$$B_d \to J/\psi + K_s \qquad \text{or} \qquad B_d \to D_u^0 \pi^0, \tag{16.36}$$

with the couplings $V_{cb}^* V_{cs}$ and $V_{cb}^* V_{ud}$, respectively.

https://doi.org/10.1017/9781009402378.017 Published online by Cambridge University Press

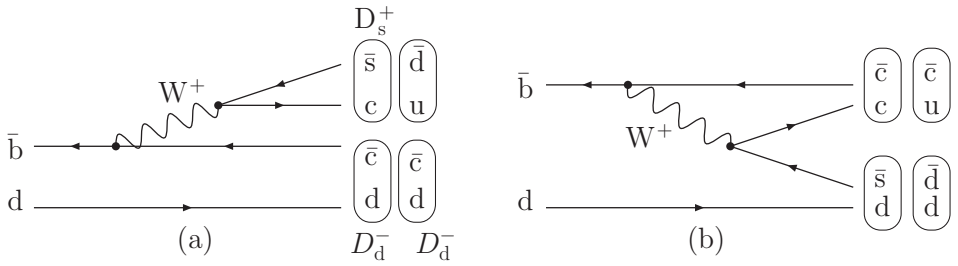

Figure 16.2. Tree-diagram decays of B_d^0.

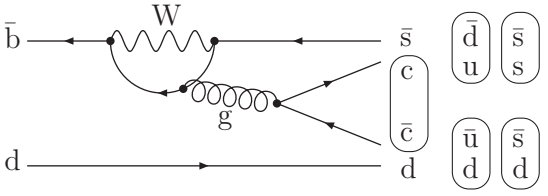

Figure 16.3. A gluonic penguin diagram.

In addition to the tree diagrams, there are penguin diagrams analogous to the ones we discussed in the previous chapter. A typical diagram for gluonic decays is shown in Fig. 16.3.

The final state is determined by the quark assignments. They can produce the following states:

$$B_d \to J/\psi + K_s, \quad B_d \to \phi K_s, \tag{16.37}$$

$$B_d \to \pi^+\pi^-, \ \pi^0\pi^0. \tag{16.38}$$

We see that the $J/\psi + K_s$ decay can originate from tree and penguin diagrams whose dynamics are very different. The dominant penguin diagrams are those with charm and top quarks in the intermediate states (see Problem 4) whose couplings are

$$V_{cb}^* V_{cs} = A\lambda^2 + O(\lambda^4), \tag{16.39}$$

and

$$V_{tb}^* V_{ts} = -A\lambda^2, \tag{16.40}$$

respectively. This CKM coupling can be extracted as a multiplicative factor. The property is unique to this decay channel and makes the predictions very reliable. For this reason the decay has been named the gold-plated decay channel. The mode has several advantages.

(i) The prediction for the CP asymmetry is reliably expressed in terms of CKM parameters and is large.

https://doi.org/10.1017/9781009402378.017 Published online by Cambridge University Press

(ii) It has a measurable branching ratio

$$\mathrm{Br}(\mathrm{B} \to \mathrm{J}/\psi \mathrm{K}^0) = (8.7 \pm 0.5) \times 10^{-4}, \tag{16.41}$$

with the decays $\mathrm{J}/\psi \to \pi^+\pi^-$ and $\mathrm{K}^0 \to \pi^+\pi^-$ producing hadrons, which are easily detectable.

(iii) The final state $\mathrm{J}/\psi + \mathrm{K_s}$ is a CP eigenstate.

For these reasons the decay of B^0 mesons to $\mathrm{J}/\psi + \mathrm{K_s}$ is an attractive mode and we describe the decay amplitudes in Problem 4.

Fortunately there is also an experimental method for detecting CP-violating effects (Carter and Sanda, 1981; Bigi and Sanda, 1981). A $\mathrm{B}^0\bar{\mathrm{B}}^0$ pair is produced in electron–positron colliders and proceeds to decay. We select a decay mode for B^0 and $\bar{\mathrm{B}}^0$ to a common final state $|f\rangle$, which is an eigenstate of CP. Let

$$A_\mathrm{f} = \langle f|H|B^0\rangle \qquad \text{and} \qquad \bar{\mathrm{A}}_\mathrm{f} = \langle f|H|\bar{B}^0\rangle$$

be the decay amplitudes. Since the beams of particles created in the collider are a mixture of B^0 and $\bar{\mathrm{B}}^0$ and since their lifetimes are almost identical, we cannot a priori tell whether $|f\rangle$ arose from the decay of B^0 or $\bar{\mathrm{B}}^0$. Thus we need independent information on the flavor of the decaying neutral B^0 meson. This can be achieved by observing a semileptonic decay on one side and the decay to $|f\rangle$ on the other side. In this way we know whether the decay to $|f\rangle$ originates from a B^0 or $\bar{\mathrm{B}}^0$. The experimental groups measure these decays as a function of time. A small asymmetry in the time evolution of the two decays is evidence for CP violation.

We describe the time evolution of particle and antiparticle decays in detail. The decay amplitudes as a function of time are

$$\langle f|B^0(t)\rangle = \frac{1}{2}\left[f_+(t)\,A_\mathrm{f} + \frac{q}{p} f_-(t)\bar{A}_\mathrm{f}\right], \tag{16.42}$$

$$\langle f|\bar{B}^0(t)\rangle = \frac{1}{2}\left[f_-(t)\,A_\mathrm{f} + \frac{q}{p} f_+(t)\bar{A}_\mathrm{f}\right]. \tag{16.43}$$

The amplitude A_f is the expectation value of the quark operators between $|B\rangle$ and $\langle f|$ states. It is computed with the help of quark diagrams described at the beginning of this section. They have a weak phase coming from the CKM-matrix elements and perhaps a phase of strong origin from final-state interactions. We shall denote the ratio

$$\rho = \frac{\bar{A}_\mathrm{f}}{A_\mathrm{f}}. \tag{16.44}$$

In the case of the B^0 mesons the factors $f_\pm(t)$ simplify, because

$$\Gamma_\mathrm{H} = \Gamma_\mathrm{L} = \Gamma$$

https://doi.org/10.1017/9781009402378.017 Published online by Cambridge University Press

and

$$f_{\pm}(t) = \mathrm{e}^{-\frac{1}{2}\Gamma t}\left(\mathrm{e}^{-\mathrm{i}M_{\mathrm{H}}t} \pm \mathrm{e}^{-\mathrm{i}M_{\mathrm{L}}t}\right). \tag{16.45}$$

The rate for detecting a decay to $|f\rangle$ at a time t after the production of a B^0 is proportional to

$$\Gamma(t) \approx \frac{1}{2}\mathrm{e}^{-\Gamma t}[1 - S_{\mathrm{f}}\sin(\Delta m\, t) + C_{\mathrm{f}}\cos(\Delta m\, t)] \tag{16.46}$$

and, for the detection of a decay from an initial $\bar{\mathrm{B}}^0$,

$$\bar{\Gamma}(t) \approx \frac{1}{2}\mathrm{e}^{-\Gamma t}[1 + S_{\mathrm{f}}\sin(\Delta m\, t) - C_{\mathrm{f}}\cos(\Delta m\, t)], \tag{16.47}$$

with

$$S_{\mathrm{f}} = \frac{2\,\mathrm{Im}\left(\dfrac{q}{p}\rho\right)}{1 + \left|\dfrac{q}{p}\rho\right|^2} \qquad \text{and} \qquad C_{\mathrm{f}} = \frac{1 - \left|\dfrac{q}{p}\rho\right|^2}{1 + \left|\dfrac{q}{p}\rho\right|^2}. \tag{16.48}$$

In both of these equations there is a time-oscillation superimposed on the exponential decay. The formulas are very general and can be applied to several decays. We consider some decays in detail.

(a) The gold-plated channel. For the decay $\mathrm{B} \to \mathrm{J}/\psi + \mathrm{K_s}$ there are tree and penguin diagrams. As we discussed in this section, all dominant diagrams have zero CKM phase (see Eqs. (16.36) and (16.39)). In addition, q/p is given by Eq. (16.13) and we obtain

$$S_{\mathrm{f}} = -\sin(2\beta), \qquad C_{\mathrm{f}} = 0$$

and

$$\Gamma(t) \approx \mathrm{e}^{-\Gamma t}[1 + \sin(2\beta)\sin(\Delta m\, t)]. \tag{16.49}$$

Thus the time evolution of the $\mathrm{B}^0_{\mathrm{d}}$ state and its conjugate particle to a common final state is an efficient method for identifying CP parameters. The asymmetry

$$\alpha = \frac{\Gamma(t) - \bar{\Gamma}(t)}{\Gamma(t) + \bar{\Gamma}(t)} = \sin(2\beta)\sin(\Delta m\, t) \tag{16.50}$$

has a sinusoidal dependence on time. This decay has been measured in the BaBar and Belle experiments, giving the average value

$$\sin(2\beta) = 0.73 \pm 0.03. \tag{16.51}$$

The angle β extracted from the asymmetry is one of the angles in the unitarity triangle. It enters the calculation through the element V_{td} given in Eq. (9.53).

The unitarity triangle is constrained by other measurements as well; to be precise, by the magnitude of V_{ub}, the parameter ε_k, and the mixing of $\mathrm{B_d}$ and $\bar{\mathrm{B}}_{\mathrm{d}}$ states. Each of these quantities determines a region and their intersection defines the apex of the

https://doi.org/10.1017/9781009402378.017 Published online by Cambridge University Press

triangle. This figure has become very popular and is featured in Fig. 9.2 and in many articles (Branco *et al.*, 1999; Kleinknecht, 2003; Brower and Faccini, 2003). The value of β in Eq. (16.51) has several solutions and one of them coincides with a direction that goes through the apex of the triangle. The significance of the $\sin(2\beta)$ measurement is that for the first time a large CP asymmetry has been observed, proving that CP is not an approximate symmetry of nature.

(b) Decays to $\pi^+\pi^-$ and $\pi^0\pi^0$. The $B \to \pi\pi$ decays can be analyzed in a similar manner to the $K \to \pi\pi$ decays. For the sake of brevity we shall use a similar notation; however, the numerical values for the quantities (amplitudes, phases, etc.) in B decays are different. The amplitude for $B^0 \to \pi^+\pi^-$ is written as

$$A_f(\pi^+\pi^-) = \sqrt{\frac{2}{3}}|A_0|e^{i(\delta_0-\theta_0)} - \frac{2}{\sqrt{3}}|A_2|e^{i(\delta_2-\theta_2)} \tag{16.52}$$

and

$$\bar{A}_f(\pi^+\pi^-) = \sqrt{\frac{2}{3}}|A_0|e^{i(\delta_0+\theta_0)} + \frac{1}{\sqrt{3}}|A_2|e^{i(\delta_2+\theta_0)}. \tag{16.53}$$

The phases δ_0 and δ_2 come from strong interactions of the final states, but at this high energy they cannot be related to $\pi\pi$ phase shifts. The phases θ_0 and θ_2 come from weak interactions, which originate from CKM couplings. The tree diagram contributes to both the $I = 0$ and the $I = 2$ amplitude and the penguin diagram only to the $I = 0$ amplitude.

The attempt to determine the isospin amplitudes by comparing decays of charged and neutral B mesons has met with limited success. This approach is analogous to that for the $K \to \pi\pi$ decays, in which, after the isospin analysis of the amplitudes, we had to return to the effective QCD Hamiltonian.

There are also analyses in terms of Feynman diagrams. We have already noted that this decay mode receives contributions from tree and penguin diagrams. In the Wolfenstein parametrization all diagrams are of order λ^3. The tree diagram has the phase $e^{-i\gamma}$. The penguin diagrams have intermediate states with up, charm, and top quarks, each with a different phase. The relevant parameter for this decay has the general form

$$\frac{q}{p}\frac{A_f(\pi^+\pi^-)}{\bar{A}_f(\pi^+\pi^-)} = e^{-2i\beta}\frac{e^{-i\gamma} + he^{i\theta}}{e^{+i\gamma} + he^{i\theta}}, \tag{16.54}$$

with h being the ratio of a term from the penguin diagram to the remaining contributions and θ a phase of strong origin. The interference of mixing with the decay amplitude gives

$$S_f(\pi^+\pi^-) \neq 0 \qquad \text{and} \qquad C_f(\pi^+\pi^-) \neq 0. \tag{16.55}$$

Consequently, the presence of both $\cos(\Delta m\, t)$ and $\sin(\Delta m\, t)$ terms with coefficients different from zero is an indication of CP violation in the B amplitudes. For very small values of h, this mode fixes

$$S_f = \sin(2\beta + 2\gamma),$$

https://doi.org/10.1017/9781009402378.017 Published online by Cambridge University Press

which, through the triangle relation $\beta + \gamma = \pi - \alpha$, can be replaced by α. Thus this decay mode can determine $\beta + \gamma$ and, indirectly, the angle α.

(c) Decays to other channels. In the previous discussion we demonstrated that β is accurately determined and γ, or alternatively α, can be extracted from the $B \to \pi\pi$ decay, provided that the hadronic matrix elements are better understood. There are extensive efforts to analyze and understand other decay modes. For instance (Fleischer, 2003),

$$B \to \phi + K_s$$

has only penguin contributions. An analysis similar to that of the $J/\psi K_s$ mode reveals many similarities. In the absence of new physics, the asymmetries for charmonium and ϕ-meson decays should be equal.

This heralds a new era, in which the theory is expected to be scrutinized through a variety of other B_d and B_s decay asymmetries. Impressive progress is being made in the search for asymmetries in the aforementioned modes and in addition $B^{0\pm} \to K\pi$ and $B^{\pm} \to DK^{\pm}$. Current measurements are approaching the stage of cross-checking the theory or even discovering physical phenomena beyond the standard model.

16.6 Mass and lifetime differences for B_s mesons

The analysis of the previous sections can be extended in a straightforward way to the B_s mesons, which present a very interesting mesonic system. Their masses and lifetimes are very similar to those of the B_d mesons, but their weak interactions are different because the CKM couplings are now much bigger. A consequence is the larger mixing in these states and, it is hoped, a lifetime difference between two physical particles that may be measurable. The reduced matrix element is given now as

$$X_{B_s} = \frac{8}{3}|\langle B_s^0|\,\bar{b}\gamma_\mu(1-\gamma_5)s|0\rangle|^2 B_s \tag{16.56}$$

and is expected to have a numerical value close to X_{B_d} because the wave functions and the general structure of the bound state are expected to be similar. The coupling which appears in the box diagrams is

$$\xi_t' = V_{tb}V_{ts}^* = -A\lambda^2, \tag{16.57}$$

which is much larger than the coupling in Eq. (16.27). The mass difference is given by a formula analogous to Eq. (16.26) and, on taking the ratio, one obtains

$$\frac{\Delta M_s}{\Delta M_d} = \frac{F_s^2}{F_d^2}\frac{M_s}{M_d}\left|\frac{V_{ts}}{V_{td}}\right|^2. \tag{16.58}$$

The ratio of the hadronic matrix parameters is unity in the SU(3) limit or the heavy-quark limit. A small deviation from unity may still show up, but this will be of order

https://doi.org/10.1017/9781009402378.017 Published online by Cambridge University Press

10%–20%. The large change comes from the couplings

$$\left|\frac{V_{ts}}{V_{td}}\right|^2 = \frac{1}{\lambda^2\left[(1-\rho)^2+\eta^2\right]} = 20\text{–}30. \tag{16.59}$$

At present there is an experimental bound, $\Delta M_s/\Delta M_d > 21.2$, coming from the mixing of B_s^0 and $\bar{B}_s^0$-particles, which is close to 100%. Serious experimental efforts are being devoted to searching for a precise value of the mixing, which will also determine the ratio $x_s = \Delta M/\Gamma$. Since the mixing approaches 100%, a precise measurement is required in order to extract a value for the mass difference (see Eq. (16.23)).

The estimate which makes x_s large also increases the width difference of the two states. The two B_s states can mix to form two distinct eigenstates. To a first approximation,

$$\frac{\Delta\Gamma_s}{\Delta M_s} = \frac{3}{2}\pi\left(\frac{m_b}{m_t}\right)^2 \approx 3.7\times 10^{-3} \tag{16.60}$$

has been calculated from equations analogous to Eqs. (16.26) and (16.32). The width difference can be rescaled to give

$$\left(\frac{\Delta\Gamma}{\Gamma}\right)_s = \frac{3}{2}\pi\left(\frac{m_b}{m_t}\right)^2\left(\frac{\Delta M_s}{\Delta M_d}\right)\left(\frac{\Delta M_d}{\Gamma}\right)_d\left(\frac{\Gamma_d}{\Gamma_s}\right). \tag{16.61}$$

The ratio of the mass difference was estimated in this section, and assuming $\Gamma_d \approx \Gamma_s$ leads to a width difference that is experimentally interesting. Its value is in the range 7%–14%. Alternative estimates that saturate Γ_{12} with physical intermediate states or form other ratios also give encouraging results. There is a good chance that the lifetime difference $\tau_H - \tau_L$ is 10% of the lifetime of B_d mesons. Such a large value would be measurable in the decay

$$B_s \to J/\psi + \phi.$$

Problems for Chapter 16

1. Carry out the integrals $\int_0^\infty |f_\pm(t)|^2\,dt$ and show that the last term in Eq. (16.8) follows. Hint: it is easier to integrate exponentials and then take real parts.
2. Write the matrix element for the mixing of the $B_d^0 \to \bar{B}_d^0$ system, especially the CKM couplings of the box diagram with the top quark in the intermediate states. Then prove the ratio
$$\frac{q}{p} = \left(\frac{H_{21}}{H_{12}}\right)^{\frac{1}{2}} \approx \frac{V_{td}}{V_{ts}^*}.$$
3. Calculate the amplitude for the diagram in Fig. 16.1(a) with charm and up quarks in the intermediate states. Then integrate over the two-body phase space to obtain some of the terms in Eq. (16.30).

https://doi.org/10.1017/9781009402378.017 Published online by Cambridge University Press

4. The decay $B_d \to J/\psi + K_s$ has tree and penguin diagrams. We denote the tree diagram by

$$T = V_{cb}^* V_{cs} g$$

and the penguin diagram by

$$P = V_{tb}^* V_{ts} f(m_t) + V_{cb}^* V_{cs}\, f(m_c) + V_{ub}^* V_{us} f(m_u),$$

where $f(m_q)$ are functions from the calculation of the penguin diagram with m_q the mass of the q quark in the loop. A naive order-of-magnitude estimate of the tree and loop diagrams gives (Gronau, 1992)

$$\frac{f(m_t)}{g} \sim \frac{\alpha_s(m_b)}{6\pi} \ln\left(\frac{m_t}{m_b}\right) \sim 0.04.$$

Others obtained larger values by computing the penguins with the effective Hamiltonian (Kramer and Palmer, 1995).

(i) Use the unitarity of the CKM matrix to eliminate $V_{tb}^* V_{ts}$ and rewrite P in terms of the other two CKM factors.

(ii) Show that the ratio of the two CKM factors is

$$\left|\frac{V_{ub}^* V_{us}}{V_{cb}^* V_{cs}}\right| \sim \lambda^2 + O(\lambda^4).$$

Prove that the total amplitude

$$\langle J/\psi K_s | H | B \rangle = V_{cb}^* V_{cs}[g + (f(m_c) - f(m_t))],$$

which to order λ^2 is real.

(iii) Use this form of the matrix element to calculate the asymmetry in Eq. (16.50).

5. Analyze the $B \to \phi + K_s$ decay along the lines of Problem 4 and derive Eq. (16.54) with an explicit expression for the function h.

References

Bigi, I. I., and Sanda, A. I. (1981), *Nucl. Phys*. **B193**, 85

Branco, G., Lavoura, L., and Silva, J. P. (1999), *CP Violation* (Oxford, Oxford University Press), Section 18.5

Brower, T. E., and Faccini, R. (2003), *Ann. Rev. Nucl. Particle Sci*. **53**, 353

Carter, A. B., and Sanda, A. I. (1981), *Phys. Rev*. **D23**, 1527

Fleischer, R. (2003), hep-ph/0310313

Gronau, M. (1992), *Phys. Lett*. **B300**, 163; hep-ph/9209279

Hagelin, J. (1981), *Nucl. Phys*. **B193**, 123

Kleinknecht, K. (2003), *Uncovering CP Violation (Experimental Classification in the Neutral K Meson and B Meson Systems)* (Springer Tracts in Modern Physics) (Berlin, Springer-Verlag), pp. 130–135

Kramer, G., and Palmer, W. (1995), *Phys. Rev*. **D52**, 6411

Paschos, E. A. and Türke, U. (1989), *Phys. Rep*. **178**, 145–260

Select bibliography

The books recommended in Chapter 15 discuss many properties of D and B mesons.

https://doi.org/10.1017/9781009402378.017 Published online by Cambridge University Press